

**Superconductivity and microstructure of  $\text{YSr}_2\text{Cu}_3\text{O}_{6.875}$** 

O. I. Lebedev\* and G. Van Tendeloo

*EMAT, University of Antwerp (RUCA), Groenenborgerlaan 171, B-2020 Antwerp, Belgium*

F. Licci, E. Gilioli, A. Gauzzi, A. Prodi, and M. Marezio

*CNR-IMEM, Parco Area delle Scienze 37/A, 43010 Fontanini-Parma, Italy*

(Received 19 June 2002; published 28 October 2002)

The crystal structure of  $\text{YSr}_2\text{Cu}_3\text{O}_{6+x}$  synthesized under high pressure has been studied in detail using transmission electron microscopy and powder neutron diffraction. It has been shown that  $\text{YSr}_2\text{Cu}_3\text{O}_{6+x}$  and  $\text{YBa}_2\text{Cu}_3\text{O}_{6+x}$  are not isostructural after all. The much lower  $T_c$  of  $\text{YSr}_2\text{Cu}_3\text{O}_{6+x}$  (YSCO) with respect to that of  $\text{YBa}_2\text{Cu}_3\text{O}_{6+x}$  has to be ascribed to the different structural arrangement of the reservoir blocks. The different oxygen ordering and the consequent displacement of the Sr and Cu1 cations in YSCO yield an orthorhombic modulated structure with a propagation vector of  $1/4[012]^*$ . Perfectly ordered YSCO would have an oxygen stoichiometry equal to 6.875. Powder neutron-diffraction data yielded  $\text{O}_{7.20}$  and  $\text{O}_{6.92}$  for the as-prepared and annealed phases, respectively.

DOI: 10.1103/PhysRevB.66.132510

PACS number(s): 74.72.Bk, 61.12.Ld, 68.37.Lp, 82.40.Fp

After the discovery of  $\text{YBa}_2\text{Cu}_3\text{O}_7$  (YBCO),<sup>1</sup> several groups tried to prepare the Sr counterpart  $\text{YSr}_2\text{Cu}_3\text{O}_z$  (YSCO). However, YSCO could only be synthesized under high pressure and  $T_c$  did not rise above 56 K.<sup>2</sup> In 1987, Cava *et al.* (Ref. 3) observed an 8 K  $T_c$  increase, when Sr replaced Ba in  $\text{La}_{1.85}\text{Ba}_{0.15}\text{CuO}_4$ . Simultaneously, Chu *et al.* (Ref. 4) observed a 12 K  $T_c$  increase when the same material was subjected to a mechanical pressure of 1 GPa. Later Locquet *et al.* (Ref. 5) reported that the  $T_c$  of a  $\text{La}_{1.9}\text{Ba}_{0.1}\text{CuO}_4$  sample increased from 25 K, as measured for a bulk sample, to 49 K, as measured for a thin film deposited on a substrate made of  $\text{SrLaAlO}_4$  with a smaller lattice parameter than the superconductor. These results strongly indicated that pressure, either mechanical, chemical or resulting from strain, can increase  $T_c$  of the high-temperature superconductors (HTS) materials.

As soon as it was known that the  $\Delta T_c / \Delta P$  coefficients for the Hg-based cuprate superconductors exhibited record breaking values,<sup>6–8</sup> numerous experiments were carried out to simulate the mechanical pressure effect by cation or anion substitutions inducing a chemical pressure. It was very disappointing to find out that the two pressures, except for the doped- $\text{La}_2\text{CuO}_4$  system and perhaps for  $\text{YBa}_2\text{Cu}_4\text{O}_8$ , had opposite effect on the critical temperature. This opposite effect can be qualitatively explained by the different effect that the two pressures have on the interatomic distances. If one examines in detail the data published for the YBCO system, one sees that in the case of the mechanical pressure, all distances decrease with increasing pressure. The  $\Delta d / \Delta P$  coefficients are all negative, even though they may vary in some cases by a factor of 2.<sup>9</sup> The corresponding values  $\Delta d / \Delta x$ , in which  $x$  represents the substitution concentration or the chemical pressure, vary over a much larger range, and some of them are positive.<sup>10</sup> This means that the effect of the chemical pressure is highly anisotropic. Because the structure is very complicated, it is not easy to single out the structural feature, which is responsible for this large anisotropy. A try was made to decrease the anisotropy by a double substitution (Yb for Y), but this resulted in an additional decrease of  $T_c$ .<sup>11</sup>

The different behavior between  $\text{La}_{1.85}\text{Ba}_{0.15}\text{CuO}_4$  and the other cuprates can be explained qualitatively in terms of the simpler structure of the former with respect to that of the latter compounds.

As stated above, even though  $\text{YSr}_2\text{Cu}_3\text{O}_{6+x}$  is the Sr counterpart of YBCO, it can only be prepared under a very high pressure.<sup>2,12,13</sup> This sort of instability indicates that the YBCO structure cannot “breathe,” preventing the total substitution of Ba with a smaller cation such as Sr. At high pressure the Ba sites become smaller. When they become too small, a phase transition may occur and in the new structure the Ba coordinates may increase. This can occur because anions are more compressible than cations. It is possible that under pressure the coordination number of the Sr cations is larger than 10, that is, larger than that of Ba in fully oxygenated YBCO at ambient pressure. As the pressure is released, the extra oxygen atoms leave the structure, but those left occupy partially both sites of the basal plane, that is, O4 and O5, in a disordered fashion, and the symmetry appears to be tetragonal by x-ray, neutron or electron diffraction. When the as-prepared (AP) samples are annealed at a rather low temperature (290 °C), a slight increase (4 K) of  $T_c$  is observed. Even though the average symmetry is still tetragonal, electron diffraction and high-resolution electron microscopy show that the symmetry has become orthorhombic. Furthermore, the structural model deduced from the observed modulation shows that the anion sublattice in YSCO and YBCO are not identical. In the present paper, we describe the experimental results that led us to demonstrate that the reservoir blocks in the two structures have different oxygen arrangements.

The  $\text{YSr}_2\text{Cu}_3\text{O}_w$  phase was obtained as an almost single-phase material (>90%) by high-pressure synthesis carried out in the presence of an oxidizing agent.<sup>13</sup> The resistivity vs temperature plots along with those of the susceptibility for the AP materials are shown in Fig. 1(a). A 1–5 °C  $T_c$  increase and the narrowing of the superconducting transition [see Fig. 1(b)] was obtained by annealing the AP samples placed in a sealed quartz ampoule at  $\approx 2$  atm oxygen pressure and 290 °C for 10 h. Hereafter, such oxygenated samples are

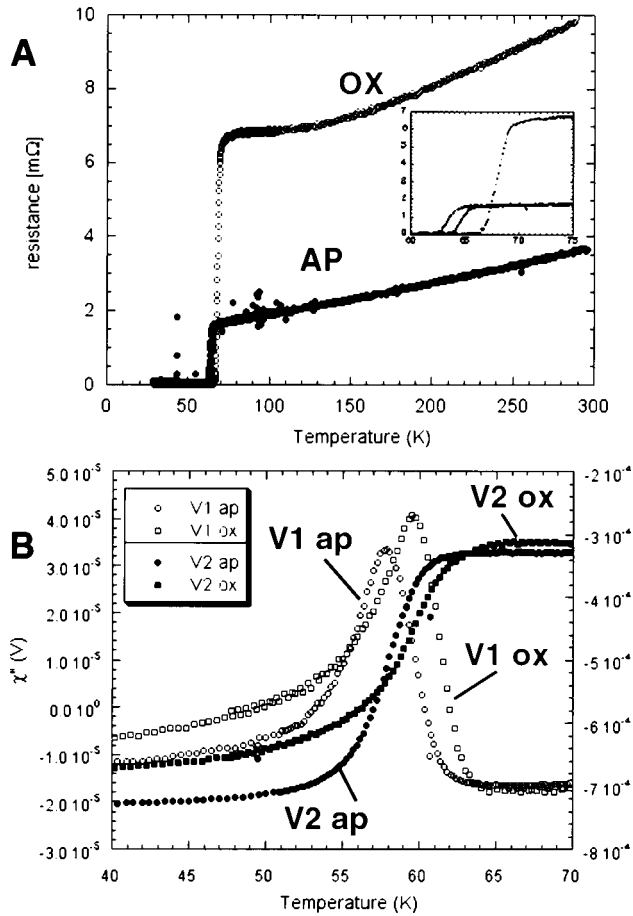


FIG. 1. Resistance (a) and susceptibility (b) of YSCO of as-prepared (in blue color—AP) and oxidized (in red color—OX) samples. The V1 and V2 are the out-of-phase and in-phase components of the voltages induced in the sensing coils of the susceptometer, as measured by the lock-in amplifier. They are proportional to the ac susceptibility. V1 is proportional to the imaginary part of susceptibility ( $\chi''$ ) whereas V2 is proportional to the real part of the susceptibility ( $\chi'$ ). The voltage values indicated on the y axes are not absolute.

indicated as OX. Paradoxically, the neutron powder-diffraction data clearly indicated that the oxygen content in OX samples was lower than in the corresponding AP samples.<sup>14</sup> The latter samples were found to be tetragonal ( $P4/mmm$ ) with  $a=b=0.37903$  nm,  $c=1.13992$  nm, and  $x=1.2$ . The structural refinement in the OX samples based on neutron-diffraction data revealed that the oxygen content decreased to 6.92. Thus, the formula had changed from  $\text{YSr}_2\text{Cu}_3\text{O}_{7.20}$  to  $\text{YSr}_2\text{Cu}_3\text{O}_{6.92}$ . We hypothesized that the AP samples were overdoped with respect to the oxygen concentration. The more stable structure resulted from the elimination of the oxygen excess at 290 °C and  $\approx 2$  atm oxygen.

The AP and OX samples were characterized and their structure determined by electron diffraction (ED) and high-resolution electron microscopy (HREM). ED patterns along the main zones confirm the tetragonality of the AP samples with a  $c/a$  ratio of 3.01. The ED patterns along the different zone axes are very much resembling the YBCO structure [Fig. 2(a)]. Also the corresponding HREM images are very

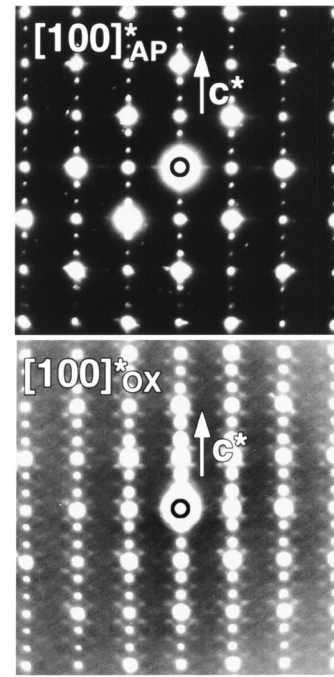


FIG. 2. [100] electron-diffraction patterns of the AP and the OX samples. The basic reflections are similar for both phases, but the OX pattern clearly shows extra satellites.

similar to the images of a YBCO-type structure [Fig. 3(a)]. Instead, the OX samples are mostly a mixture of a tetragonal and an orthorhombic phase. It is important to notice that the  $c/a$  ratio of the OX is 2.95, namely smaller than that of the AP. The orthorhombic structure is also characterized by a weak modulation with a wave vector  $q \approx 1/4 [012]^*$ , visible in a [100] section [Fig. 2(b)]. The corresponding HREM image shows the basic image with a modulation superimposed to the basic structure (Fig. 3). Apart from the modulation, the image is very similar to that of the nonmodulated AP phase, indicating that the cation positions have hardly changed. Around the Cu1 layers (identified from image simulations), one notices four brighter dots at regular intervals, comprising two Cu1 and two Sr cations. These clusters of four dots seem to form a defect occurring after every four basic units along the  $b$  direction and every two along  $c$ . The modulation is related to the formation of a superstructure with lattice parameters  $a_{ss} \approx a_T$ ,  $b_{ss} \approx 4a_T$ , and  $c_{ss} \approx 2c_T$  (see Fig. 4). With respect to the unmodulated AP phase, the  $c$  parameter (i.e.,  $c_{ss}/2$ ) is slightly decreased. The reason why the diffraction pattern shows a modulated structure rather than a full superstructure is related to the fact that the modulation is domain fragmented. The size of these domains is in the nanometer scale.

A similar modulation was observed before in YBCO-based materials, and was found to be associated with the presence of anion groups such as  $\text{CO}_3$  or  $\text{SO}_4$  (Refs. 15–17) replacing Cu1. In the present study, the AP samples were accurately tested by Auger electron microscopy and no contamination by carbonates was detected ( $<1\%$ ). Therefore, we have to assume that the modulation is intrinsic to the orthorhombic structure of  $\text{YSr}_2\text{Cu}_3\text{O}_x$ . Since the modulation

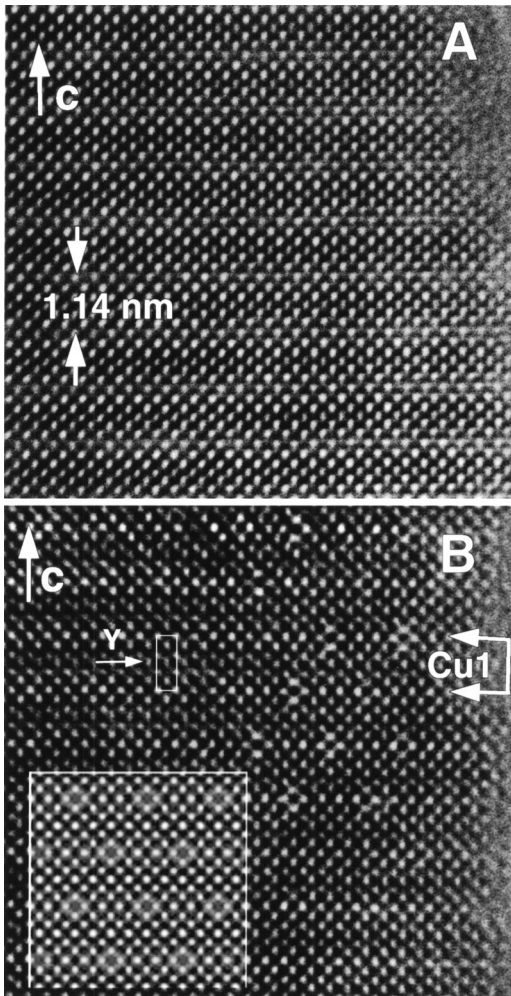


FIG. 3. HREM images along  $[100]$ , corresponding to the diffraction patterns of Figs. 2(a) and 2(b). Experimental conditions are such that the bright dots image the cations in the structure. In (b), four brighter dots, comprising two Cu1 and two Sr cations are formed at regular intervals. The inset shows the simulated image obtained at a defocus value  $\Delta f = -20$  nm and thickness  $t = 8$  nm, based on the structure proposed in Fig. 4.

is absent in the AP samples, the oxygen rearrangement induced by heat treatment seems to be essential for the superstructure formation.

Image simulations of the modulated structure, based on a  $P4/mmm$  symmetry, reveal that the distortion related to the formation of the superstructure is located around the Cu1 sites. This observation is in agreement with the structural refinements of the AP and OX phases based on powder neutron-diffraction data.<sup>14</sup> These refinements clearly show that the reservoir block (SrO) (CuO) (SrO) around the Cu1 layer is more disordered than the superconducting block (CuO<sub>2</sub>)Y(CuO<sub>2</sub>). This was deduced from the values of the Debye-Waller (DW) factors and the standard deviations of both the positional and DW factors. In the OX samples, the Sr thermal factors are much larger than those of Y ( $U_{eq} = 0.0161(7) \text{ \AA}^2$  for Sr as compared to  $0.0022(6) \text{ \AA}^2$  for Y), while for the AP samples they are comparable (Table I). This indicates that the modulated phase is associated with a Sr

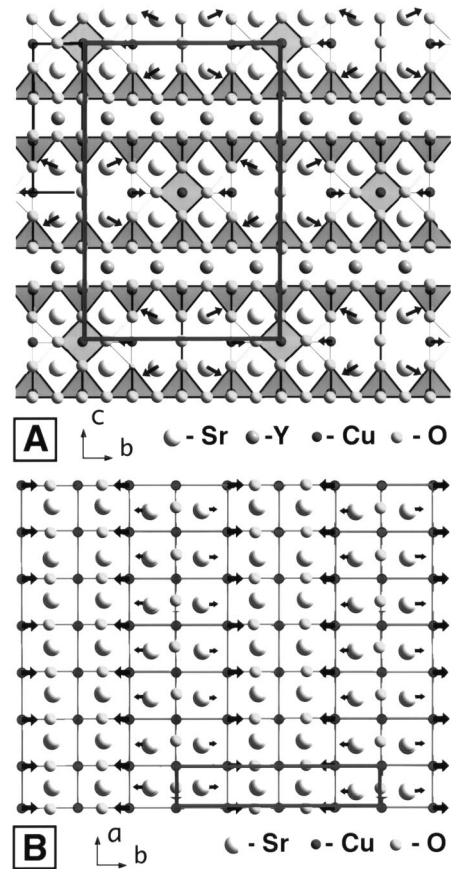


FIG. 4. Structural model of the orthorhombic YSCO, taking into account all experimental evidence; A represents the projection on  $b$ - $c$  plane; B represents the projection on  $a$ - $b$  plane.

displacement from the ideal position of the  $P4/mmm$  symmetry. Since oxygen vacancies and/or displacements barely influence the HREM contrast, the brighter spots should be linked to cation displacements. These displacements, however, are induced by the oxygen rearrangement taking place during the heat treatment.

To explain these observations we analyzed a number of different models, corresponding to different cation displace-

TABLE I. Thermal factors and statistical indicators of the Rietveld refinement of the powder neutron-diffraction data relevant to AP and OX YSCO samples. wRp and Rp indicate respectively the weighted and nonweighted pattern regression factors.

	OX sample	AP sample
	$U_{eq} (\text{\AA}^2)$	$U_{11}, U_{22}, U_{33} (\text{\AA}^2)$
Sr	0.0161(7)	0.0143(11), 0.0143(11), 0.0218(19)
Cu1	0.0164(9)	0.0295(16), 0.0295(16), 0.0003(18)
Y	0.0024(6)	0.0058(7), 0.0058(7), 0.0058(7)
O1	0.0136(11)	0.0322(20), 0.0322(20), 0.0061(21)
O4	0.0218(38)	0.1347(362), 0.0305(62), 0.0095(52)
wRp	0.0380	0.0402
Rp	0.0354	0.0342
$\chi^2$	9.526	17.41

ments around the Cu1. The only model able to reproduce the experimental HREM images of Fig. 3(b) is shown in Fig. 4(a). Eight Sr positions and two Cu1 neighbors are slightly displaced along the  $[012]$  direction and the  $b$  axis, respectively. The simulated HREM image (for displacements of 0.2 Å) [inset of Fig. 3(b)] shows a striking agreement with the experimental image.

To locate the oxygen atoms in the basal plane, we have to take into account all experimental data (neutron diffraction as well as electron microscopy) for both the AP and the OX phase.

(1) The structural refinement indicates that the AP phase is tetragonal. The oxygen atoms are distributed over the two equivalent sites O4 (0,1/2,0) and O5 (1/2,0,0). The oxygen stoichiometry as deduced from the oxygen occupancy factors is 7.20. The average coordination number of Cu1 is 4.2, which means that some Cu1 should be pyramidally coordinated. The square or pyramidal Cu1 chains run along the  $a$  or  $b$  axis. The chains are short, in agreement with the tetragonal symmetry. However, there is no clue as how short they really are.

(2) The structural refinement of the OX phase is only indicative for it has been carried out in the tetragonal space-group symmetry. In fact, it is very similar to that of the AP phase. As stated above, it only indicates that the disorder is in the reservoir block. The oxygen stoichiometry decreases to 6.92. The average coordination number of the Cu1 cations is now less than 4. Being an average structure, we cannot make any further statement.

(3) The refinements yield a larger  $c$  axis for the AP structure than for the OX one. ED shows that this is still true on a local scale.

(4) The Debye-Waller factors strongly indicate that the cation displacements responsible for the modulation, observed in the OX phase, are those contained in the reservoir blocks, namely, Sr and Cu1.

A plausible oxygen distribution in the basal plane, which would be in agreement with all the data discussed above, is shown in Fig. 4(b). The unit cell would be  $a = a_T$ ,  $b = 4a_T$ , and  $c = 2c_T$ . The number of 3-coordinated Cu1 is equal to that of the 4-coordinated Cu1. The proposed oxygen distribution would induce slight displacement of eight Sr and two Cu1 cations to new positions, which simulate perfectly the observed HREM image. It would also induce a decrease in the  $c$  parameter when the ordering takes place. Due to the loss of oxygen, the number of 3-coordinated Cu1 increases

on going from the AP to the OX phase. The apical distances corresponding to the 3-coordinated cations would have to decrease in order to compensate the loss of negative charge.

If the oxygen distribution of the OX phase is that represented in Fig. 4(b), the oxygen stoichiometry would be 6.875, which is close to that found by neutron-diffraction data (6.92). The extra 0.05 oxygen could be located on the empty O4 sites. The oxygen distribution in the ordered YSCO phase would be able to increase from 6.875 to 7.2 or to a higher value. The model proposed in Fig. 4 is in agreement with the composition, the symmetry, and the HREM images. The computer-simulated HREM image in Fig. 3(b) is based on the present model, using the experimental parameters for the microscope, a focus value of  $-20$  nm, and a crystal thickness of 8 nm; though we cannot claim that the oxygens are accurately positioned. As we mentioned before, the HREM image is only weakly dependent on the exact oxygen positions.

To explain the structural difference between YBCO and YSCO, one has to assume that the blocks ( $\text{CuO}_2\text{-Y-CuO}_2$ ) are very rigid, which seems to be the case as demonstrated by all the structural refinements carried out so far. Since the very early 1990s it was shown that the Ba layers are under severe strain. This strain seems to be induced by the rigidity of the neighboring layers. It is needed to optimize the charge transfer from the chain Cu to the planar Cu cations. It was later shown that the substitution of Sr for Ba releases the strain, and this is accompanied by a decrease of  $T_c$ . However, when the alkali-earth metal site is fully occupied by Sr, the negative strain, which is produced by the substitution, decreases. Furthermore, the orthorhombic distortion induced by the CuO chains would be larger in YSCO than in YBCO,<sup>18</sup> requiring the storage of a larger elastic energy in the structure. This is implemented by the specific oxygen distribution on the Cu1 layers. The formula of the most stable YSCO should be  $\text{YSr}_2\text{Cu}_3\text{O}_{6.875}$ . One should not need ultra-high-pressure conditions to prepare it. However, YSCO forms more easily under pressure because the latter reduces the size of the alkali-earth metal site, and these smaller sites can accommodate the Sr cations. A subsequent gentle heat treatment then induces the stable structure of YSCO.

The authors would like to thank H. J. Mathieu and N. Xanthopoulos for the Auger microscopy analysis, P. G. Radaelli for the neutron diffraction experiments, and T. H. Geballe for critically reading the manuscript. Part of this work had been performed within the framework of IUAP V-1, an initiative of the Belgian government.

\*Corresponding author.

<sup>1</sup>M. K. Wu *et al.*, Phys. Rev. Lett. **58**, 908 (1987).

<sup>2</sup>B. Okai, J. Appl. Phys. **29**, L2180 (1990).

<sup>3</sup>R. J. Cava *et al.*, Phys. Rev. Lett. **58**, 408 (1987).

<sup>4</sup>C. W. Chu *et al.*, Phys. Rev. Lett. **58**, 405 (1987).

<sup>5</sup>J. P. Locquet *et al.*, Nature (London) **394**, 453 (1998).

<sup>6</sup>C. W. Chu *et al.*, Nature (London) **365**, 323 (1993).

<sup>7</sup>M. Nunez-Regueiro *et al.*, Science **262**, 97 (1993).

<sup>8</sup>L. Gao *et al.*, Phys. Rev. B **50**, 4260 (1994).

<sup>9</sup>J. D. Jorgensen *et al.*, Phys. Rev. B **41**, 1863 (1990).

<sup>10</sup>F. Licci *et al.*, Phys. Rev. B **58**, 15 208 (1998).

<sup>11</sup>A. Prodi, A. Gauzzi, E. Gilioli, F. Licci, M. Marezio, F. Bolzoni, G. Allodi, R. De Renzi, and P. G. Radaelli (unpublished).

<sup>12</sup>Y. Cao *et al.*, Phys. Rev. B **58**, 11 201 (1998).

<sup>13</sup>E. Gilioli *et al.*, Physica C **341-348**, 605 (2000).

<sup>14</sup>A. Gauzzi *et al.* (unpublished).

<sup>15</sup>Y. Miyazaki *et al.*, Physica C **198**, 7 (1992).

<sup>16</sup>B. Domenges *et al.*, Physica C **207**, 65 (1993).

<sup>17</sup>O. Milat *et al.*, Physica C **210**, 439 (1993).

<sup>18</sup>A. Gauzzi *et al.*, Proc. SPIE **4058**, 12 (2000).